

Minimal-size Real Space d -wave Pairing Operator in CuO_2 Planes

Adriana Moreo^{1,2} and Elbio Dagotto^{1,2}

¹*Department of Physics and Astronomy, University of Tennessee, Knoxville, TN 37966, USA*

²*Materials Science and Technology Division, Oak Ridge National Laboratory, Oak Ridge, TN 37831, USA*

(Dated: September 11, 2019)

A novel minimal-size pairing operator Δ_{D0}^\dagger with d -wave symmetry in CuO_2 planes is introduced. This pairing operator creates on-site Cooper pairs at the four oxygens that surround a copper atom. Via the time evolution of Δ_{D0}^\dagger , an additional inter-orbital pairing operator Δ_{Dpd}^\dagger with d -wave symmetry is generated that pairs fermions located in a Cu and its four surrounding O's. The subsequent time evolution of Δ_{Dpd}^\dagger generates an intra-orbital d -wave pairing operator Δ_{Dpp}^\dagger involving the four O atoms that surround a Cu, as well as the d -wave operator Δ_D^\dagger traditionally used in single-band models for cuprates. Because we recover the larger size operators extensively used in the three-orbital Hubbard model, we suggest that long-range order using the canonical extended operators occurs together with long-range order in the new minimal operators. However, our minimal d -wave operators could be more practical to study d -wave superconductivity because in the finite-size relatively small systems accessible to computational techniques it is easier to observe long-range order using local operators. Moreover, an effective model with the usual tight-binding hopping of the CuO_2 planes supplemented by an attractive potential V in the d -wave channel is introduced. Using mean-field techniques we show that a paired ground state is stabilized for any finite value of V . We observed that the values of V that lead to gap sizes similar to those in the cuprates are smaller for d -wave pairing operators that include Cu d -orbitals than those that only include p -orbitals. In all cases the gap that opens in the spectrum has standard d -wave symmetry. Finally, a simpler effective model is introduced to study the phenomenology of multi-orbital d -wave superconductors, similarly as the negative- U Hubbard model is used for properties of s -wave superconductors.

PACS numbers: 74.72-h, 74.25.-q
Keywords:

I. INTRODUCTION

The discovery of d -wave superconductivity in the high critical temperature cuprates [1, 2] started efforts to develop effective Hamiltonians that would allow to study d -wave pairing in the same way as the negative- U Hubbard model allows the study of s -wave pairing in standard BCS superconductors [3–5]. Previous efforts focused on single-orbital systems with on-site Coulomb repulsion together with an effective attractive nearest-neighbors potential [6, 7], hardcore dimers [8], or via the phenomenological addition of a term proportional to the square of the nearest-neighbor hoppings [9]. These models were difficult to study, parameters needed to be fine tuned, and actual numerical evidence of long-range d -wave pairing correlations has been elusive [10]. The contribution of orbital degrees of freedom to the symmetry of the pairing operator came to the foreground when superconductivity was observed in iron-based pnictides and selenides [11–14] and recently an effective model with on-site inter-orbital attraction was presented [15]. While relatively easy to study, inter-orbital same-site pairing operators are considered to be less likely to develop long-range order than their intra-orbital counterparts involving the same orbital but at different sites. For all these reasons, it is still important to find alternative and practical intra-orbital pairing operators with d -wave symmetry.

In addition, recent angle-resolved photoemission experiments using $\text{Bi}_2\text{Sr}_2\text{CaCu}_2\text{O}_{8+\delta}$ indicated a novel

“starfish” shape of the superconducting pairs with a very short length – of the order of one lattice space – in the antinodal direction [16]. This unexpected result appears to be doping independent and it may offer clues on the local structure of d -wave pairs in the strong coupling regime. For us these experiments provide additional motivation to reconsider the local form of the d -wave pairing operators in the cuprates.

Most previous attempts to construct same-orbital effective d -wave models, analogous to the $U < 0$ Hubbard model for s -wave, relied on single-orbital systems with electrons placed on sites of a square lattice that mimic only the coppers. In the present publication, we aim to explore whether effective models for d -wave superconductivity can be constructed using, instead, the oxygen locations in the more realistic CuO_2 lattice. It is well known that holes tend to reside on oxygens due to the charge transfer nature of the cuprates. However, the vast majority of theory efforts in this context rely on one-orbital Cu-only models, such as the $t - J$ and one-orbital Hubbard. Only recently computational efforts are studying the full CuO_2 models, with both Cu and O incorporated, and interesting results such as stripes have already been unveiled in this context [17–19]. Thus, our focus and main question addressed are timely: *can we find an effective model for d -wave superconductivity using only the oxygens of a CuO_2 lattice, namely only the atoms placed at the bonds of the said square lattice?* Moreover, in searching for the most compact in size form for this pairing

operator we will address, as a bonus, the recent photoemission results in the cuprates that unveiled very small Cooper pairs, at least in the antinodal directions [16]. Our overarching goal can be framed similarly as early studies within one-orbital models that attempted to construct quasiparticle operators with a larger quasiparticle weight Z that those of the usual bare operators (i.e. better "antennas"), and thus derive pairing operators that could produce stronger signals in computational studies [20].

This paper is organized as follows: in Section II the models traditionally used to study the cuprates, as well as the d -wave pairing operators previously investigated, are discussed. Our new minimal d -wave pairing operator in the CuO_2 planes is introduced in Section III, while in Section IV additional d -wave pairing operators, including the more standard extended ones, are deduced by calculating the time evolution of the minimal operator. Both the minimal and some extended pairing operators are studied at the mean-field level in Section V and a simple effective model is introduced in Section VI. Section VII is devoted to our conclusions.

II. MODELS AND PREVIOUSLY USED d -WAVE PAIRING OPERATORS FOR CUPRATES

It is widely accepted that a realistic model to describe CuO_2 planes is a three-orbital Hubbard model that includes the $d_{x^2-y^2}$ orbitals at the coppers and the p_σ orbitals at the oxygens at a distance $\hat{\mu}/2$ from the coppers (lattice constant units), with $\hat{\mu} = x$ or y [21] i.e. along the two directions. The Hamiltonian is

$$H_{3\text{BH}} = H_{\text{TB}} + H_{\text{int}}, \quad (1)$$

where

$$\begin{aligned} H_{\text{TB}} = & -t_{pd} \sum_{\mathbf{i}, \mu, \sigma} \alpha_{\mathbf{i}, \mu} (p_{\mathbf{i}+\frac{\hat{\mu}}{2}, \mu, \sigma}^\dagger d_{\mathbf{i}, \sigma} + h.c.) - \\ & t_{pp} \sum_{\mathbf{i}, \langle \mu, \nu \rangle, \sigma} \alpha'_{\mathbf{i}, \mu, \nu} [p_{\mathbf{i}+\frac{\hat{\mu}}{2}, \mu, \sigma}^\dagger (p_{\mathbf{i}+\frac{\hat{\nu}}{2}, \nu, \sigma} + p_{\mathbf{i}-\frac{\hat{\nu}}{2}, \nu, \sigma}) + h.c.] \\ & + \epsilon_d \sum_{\mathbf{i}} n_{\mathbf{i}}^d + \epsilon_p \sum_{\mathbf{i}, \mu} n_{\mathbf{i}+\frac{\hat{\mu}}{2}}^p + \mu_e \sum_{\mathbf{i}, \mu} (n_{\mathbf{i}+\frac{\hat{\mu}}{2}}^p + n_{\mathbf{i}}^d), \end{aligned} \quad (2)$$

and

$$H_{\text{int}} = U_d \sum_{\mathbf{i}} n_{\mathbf{i}, \uparrow}^d n_{\mathbf{i}, \downarrow}^d + U_p \sum_{\mathbf{i}, \mu, \sigma} n_{\mathbf{i}+\frac{\hat{\mu}}{2}, \uparrow}^p n_{\mathbf{i}+\frac{\hat{\mu}}{2}, \downarrow}^p. \quad (3)$$

The operator $d_{\mathbf{i}, \sigma}^\dagger$ creates an electron with spin σ at site \mathbf{i} of the copper square lattice, while $p_{\mathbf{i}+\frac{\hat{\mu}}{2}, \mu, \sigma}^\dagger$ creates an electron with spin σ at orbital p_μ , where $\mu = x$ or y , for the oxygen located at $\mathbf{i} + \frac{\hat{\mu}}{2}$. The hopping amplitudes t_{pd} and t_{pp} correspond to the hybridizations between nearest-neighbors Cu-O and O-O, respectively, and $\langle \mu, \nu \rangle$

indicate O-O pairs connected by t_{pp} as shown in Fig. 1. $n_{\mathbf{i}+\frac{\hat{\mu}}{2}, \sigma}^p$ ($n_{\mathbf{i}, \sigma}^d$) is the number operator for p (d) electrons with spin σ , and ϵ_d and ϵ_p are the on-site energies at the Cu and O sites, respectively. The Coulomb repulsion between two electrons at the same site and orbital is U_d (U_p) for d (p) orbitals. The signs of the Cu-O and O-O hoppings due to the symmetries of the orbitals is included in the parameters $\alpha_{\mathbf{i}, \mu}$ and $\alpha'_{\mathbf{i}, \mu, \nu}$ and follow the convention shown in Fig. 1. Finally, μ_e is the electron chemical potential. The hopping parameters are those much used for the cuprates i.e. $t_{pd} = 1.3$ eV and $t_{pp} = 0.65$ eV, on-site energy $\epsilon_p = -3.6$ eV [22], and $\Delta_{CT} = \epsilon_d - \epsilon_p$ which is positive ($\epsilon_d = 0$) [23] is the charge-transfer gap.

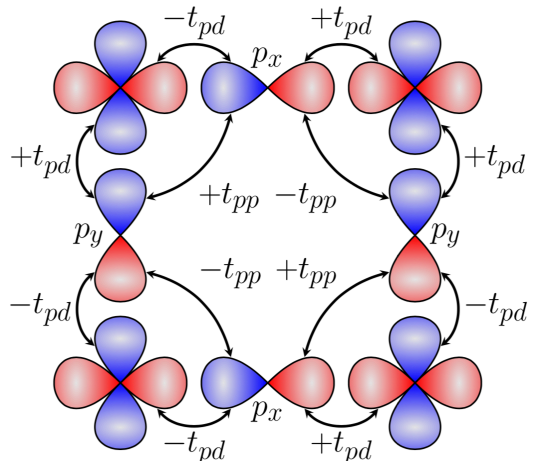


FIG. 1: (color online) Schematic drawing of the Cu $d_{x^2-y^2}$ orbitals at the copper sites of the square lattice, with the sign convention indicated by the colors (red for + and blue for -). The oxygen p_σ orbitals with their corresponding sign convention are also shown, located at the Cu-O-Cu bonds. The sign convention for the t_{pd} and t_{pp} hoppings is also presented.

A. Single-orbital d -wave operators

Because experiments indicate that the Fermi surface of the cuprates is determined by a single band [24–27], and theoretically a mapping of the three-band Hubbard model to the $t - J$ Hamiltonian can be obtained via Zhang-Rice singlets [28], using only one band is appealing. In fact, due to their relative simplicity, the study of single-orbital models has prevailed in the cuprates. As a result, the simplest pairing operators with d -wave symmetry are extended in the sense that they involve nearest-neighbor Cu sites [29, 30], without the oxygens in between. Zhang and Rice studied the addition of one hole in an undoped three-orbital Hubbard model using a CuO_4 cluster but neglecting the O-O hopping. They found that the hole occupies a symmetric linear combination involving the four O's around a Cu, and forms a spin singlet together with the hole in the central Cu [28]. They also showed that the energy of the small cluster with two extra holes in the O orbitals was higher than

the energy of two separated O holes. The next step was to construct Wannier functions combining the single-cluster symmetric single-hole plaquette states and obtain the effective single-orbital low-energy model, leading to the $t - J$ model. As discussed earlier, the simplest d -wave pairing operator in the $t - J$ (and one-orbital Hubbard) modes involves nearest-neighbor sites and has the well-known form:

$$\Delta_D^\dagger(\mathbf{j}) = \sum_{\mu,\sigma} f(\sigma)\gamma_\mu c_{\mathbf{j}+\hat{\mu},\sigma}^\dagger c_{\mathbf{j},-\sigma}^\dagger, \quad (4)$$

where $c_{\mathbf{j},\sigma}^\dagger$ creates an electron with spin σ at site \mathbf{j} of the Cu square lattice [see panel (a) of Fig. 2], $\gamma_\mu=1$ (-1) for $\mu = \pm x$ ($\pm y$) and $f(\sigma) = 1(-1)$ if $\sigma = \uparrow(\downarrow)$.

B. Three-orbital extended d -wave operators

Note that the empty sites (holes) in the effective $t - J$ model contain Zhang-Rice singlets (ZRS) which means that the components of the Cooper pair in Eq. (4) are created on top of the ZRS. The first numerical calculations studying pairing were performed in single-orbital models [29] and when, later on, pairing was numerically evaluated in three-orbital Hubbard models, the pairing operators used [18, 31, 32] were straightforward generalizations of Eq. (4) [see panel (b) of Fig. 2] involving several sites, such as

$$\begin{aligned} \Delta_{D3B}^\dagger(\mathbf{j}) = & \sum_{\mu,\sigma} f(\sigma)\gamma_\mu [d_{\mathbf{j}+\hat{\mu},\sigma}^\dagger d_{\mathbf{j},-\sigma}^\dagger + \\ & p_{\mathbf{j}+\hat{\mu}+x/2,x,\sigma}^\dagger p_{\mathbf{j}+x/2,x,-\sigma}^\dagger + \\ & p_{\mathbf{j}+\hat{\mu}+y/2,y,\sigma}^\dagger p_{\mathbf{j}+y/2,y,-\sigma}^\dagger]. \end{aligned} \quad (5)$$

This operator creates electrons that form intra-orbital pairs whose d -wave symmetry is determined by γ_μ . It considers that Cooper pairs are formed by one electron (or hole) in a Cu and another in its neighboring Cu atoms, and similarly for electrons (or holes) in the p -orbitals. It is in this sense that this operator is intra-orbital: the pair terms involve either Cu or O. In real space the minimum pair created by the pairing operators in Eqs. 4 and 5 involves five lattice sites, in a single-orbital model context, or several unit cells (21 Cu and O sites) for the three-orbital case. Such extended pairing operators [see panels (a) and (b) of Fig. 2] appear at odds with the recent experimental results of Ref. [16] where the observed pairs have a minimum real-space extension of the order of the lattice constant along the antinodal direction. This photoemission experiment offers motivation to investigate if in the CuO_2 planes it is possible to construct a more local d -wave pairing operator involving far less sites and ideally just one unit cell.

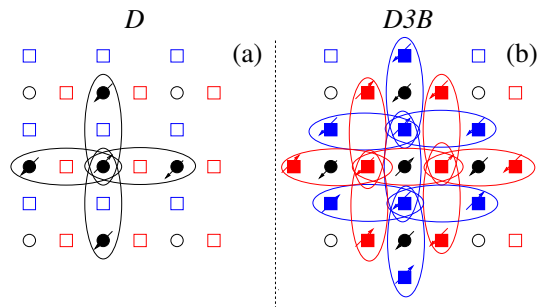


FIG. 2: (color online) Schematic drawing of previously used d -wave pairing operators in the CuO_2 planes. Circles indicate the Cu d -orbitals sites while red (blue) squares indicate the O p_x (p_y) orbitals sites. Filled symbols indicate atoms where the particles forming the Cooper pairs are located and arrows indicate the spin of the electrons/holes in the pair. (a) In single-orbital approximations to the CuO_2 planes the Cooper pairs are assumed to be primarily located in nearest-neighbor Cu sites via the operator Δ_D^\dagger . (b) In the three-orbital Hubbard model the d -wave pairing operator Δ_{D3B}^\dagger adds Cooper-pairs involving p_x and p_y orbitals, in addition to the Cu orbitals as in (a) not shown in this panel for clarity. The individual Cooper pairs are encircled with ellipses. The relative phases are positive along x and negative along y .

III. MINIMAL d -WAVE PAIRING OPERATOR

As explained, in undoped systems and in the Zhang-Rice approximation a doped hole is placed at an oxygen and forms a ZRS with the hole at a copper. A second doped hole is expected to form another ZRS with a different Cu. The one-orbital pairing operator in Eq. (4) can only involve electrons at two neighboring Cu sites, each with its own ZRS. However, in the three-orbital Hubbard model formulation there is no clear relation between the pairing operator and the two neighboring ZRS. Equation (5) just considers that the minimal Cooper pair can be formed by fermions at a d (p_σ) orbital and at the four nearest-neighbor Cu (O) atoms, thus involving five unit cells, and many sites.

As discussed above, Zhang and Rice found out that it would be unlikely that two holes would share the O orbitals of one single plaquette. However, calculations including t_{pp} hopping and the $p - d$ Coulomb repulsion, both neglected in the ZRS derivation, indicated that an effective attraction between holes in the oxygens of a single plaquette may develop [33, 34]. Thus, the possibility that two holes could form a pair in the O orbitals in a single plaquette deserves to be explored.

First, we will construct an on-site d -wave pairing operator which considers only *doubly occupied* O sites [see panel (a) in Fig. 3] in analogy with the on-site attractive s -wave pairing operator. It has the form

$$\begin{aligned} \Delta_{D0}^\dagger(\mathbf{j}) = & \frac{1}{2} \sum_{\mu,\sigma} f(\sigma)\gamma_\mu p_{\mathbf{j}+\hat{\mu}/2,\mu,\sigma}^\dagger p_{\mathbf{j}+\hat{\mu}/2,\mu,-\sigma}^\dagger = \\ & \sum_{\mu} \gamma_\mu p_{\mathbf{j}+\hat{\mu}/2,\mu,\uparrow}^\dagger p_{\mathbf{j}+\hat{\mu}/2,\mu,\downarrow}^\dagger. \end{aligned} \quad (6)$$

Although the operator involves doubly-occupied sites, each one apparently *s*-wave, since the operator involves four oxygens around the same copper, a linear combination can be made that renders the full operator *d*-wave.

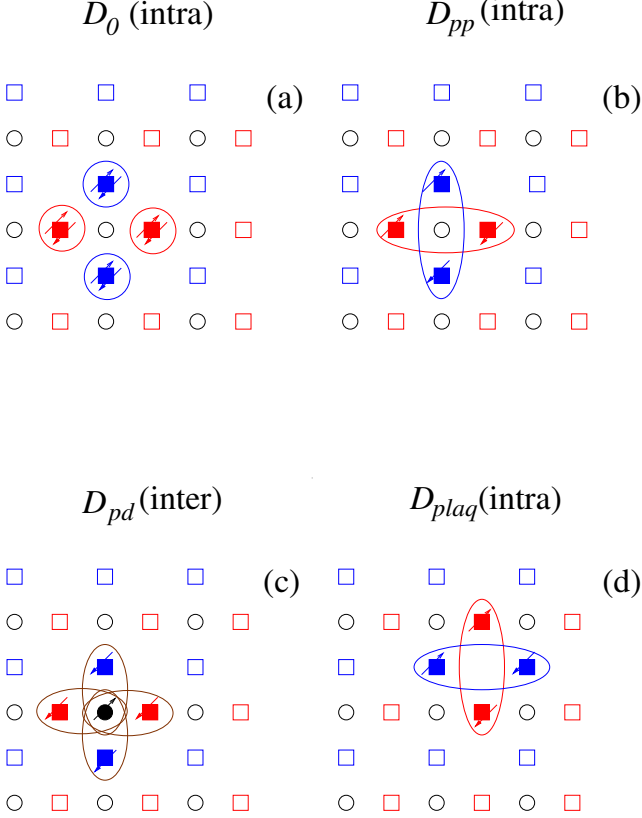


FIG. 3: (color online) Schematic drawing of the minimal intra-unit cell *d*-wave pairing operators introduced here for the CuO₂ planes, that were not explored before in three-orbital Hubbard models to our knowledge. Circles indicate the Cu *d*-orbitals while the red (blue) squares indicate the p_x (p_y) orbitals at the O atoms. Filled symbols indicate sites where the particles forming the Cooper pairs are located and arrows indicate the spin of the electrons/holes in the pair. (a) On-site intra-orbital (i.e. same oxygen) *d*-wave operator Δ_{D0}^\dagger , defined in Eq. (6). Here the two members of the Cooper pair are at the same oxygen, linearly combined involving the four possible oxygens. (b) More extended nearest-neighbor intra-orbital *d*-wave operator Δ_{Dpp}^\dagger where the Cooper pair is formed by two electrons in the same p_σ orbital, either x or y , at a distance of one lattice spacing forming a spin singlet, and linearly combining the vertical and horizontal directions to form a *d*-wave operator. (c) Inter-orbital (*dp*) *d*-wave operator Δ_{Dpd}^\dagger with pairs involving a particle at the central Cu and the other at a neighboring O, linearly combined to form a *d*-wave. (d) Plaquette *d*-wave intraorbital pairing operator Δ_{Dplaq}^\dagger in the CuO₂ plane. In (a-d), the Cooper pairs are circled with ellipses. Relative phases are positive along x and negative along y , leading to a *d*-wave.

IV. TIME-EVOLUTION OF THE PAIRING OPERATOR

In previous literature [35, 36] a relationship between the on-site and the extended *s*-wave pairing operators in the single-orbital Hubbard model was obtained by calculating the time evolution of the on-site pairing operator. Following similar steps we can now calculate the time evolution of the on-site minimal *d*-wave pairing operator Δ_{D0}^\dagger proposed in Eq. (6) for the three-orbital Hubbard model Eq. (1). We found that

$$-i \frac{d\Delta_{D0}^\dagger}{dt} = [H_{3BH}, \Delta_{D0}^\dagger] = 2(\epsilon_p - \mu_e)\Delta_{D0}^\dagger - U_p\Delta_{D0}^\dagger - t_{pd}\Delta_{Dpd}^\dagger, \quad (7)$$

where Δ_{Dpd}^\dagger is another *d*-wave pairing operator defined in one unit-cell CuO₂. Δ_{Dpd}^\dagger forms Cooper pairs with one fermion at a Cu and the other in an antisymmetric linear combination of the p_σ orbitals in its four nearest-neighbor O's [panel (c) of Fig. 3] and it is given by

$$\Delta_{Dpd}^\dagger(\mathbf{j}) = \sum_{\mu,\sigma} f_\sigma \gamma_\mu \alpha_{\mathbf{j},\mu} d_{\mathbf{j},\sigma}^\dagger p_{\mathbf{j}+\hat{\mu}/2,\mu,-\sigma}^\dagger. \quad (8)$$

Since in the ground state the average value of the pairing operators is time-independent, from Eq. (7) we see that the average values of the two pairing operators must be related. In addition, by evaluating the time evolution of the new inter-orbital minimal pairing operator, Δ_{Dpd}^\dagger , more extended intra- and inter-orbital pairing operators with *d*-wave symmetry are obtained. For example, from the commutator between Δ_{Dpd}^\dagger and the t_{pd} hopping term in H_{3BH} we obtain the nearest-neighbor *d*-orbital pairing operator in Eq. (4) depicted in panel (a) of Fig. 2 and an additional intra-orbital pairing operator given by

$$\begin{aligned} \Delta_{Dpp}^\dagger(\mathbf{j}) &= (p_{\mathbf{j}+x/2,x,\uparrow}^\dagger p_{\mathbf{j}-x/2,x,\downarrow}^\dagger - p_{\mathbf{j}+x/2,x,\downarrow}^\dagger p_{\mathbf{j}-x/2,x,\uparrow}^\dagger) - \\ & (p_{\mathbf{j}+y/2,y,\uparrow}^\dagger p_{\mathbf{j}-y/2,y,\downarrow}^\dagger - p_{\mathbf{j}+y/2,y,\downarrow}^\dagger p_{\mathbf{j}-y/2,y,\uparrow}^\dagger) = \\ & \sum_{\mu,\sigma} f_\sigma \gamma_\mu p_{\mathbf{j}+\hat{\mu}/2,\mu,\sigma}^\dagger p_{\mathbf{j}-\hat{\mu}/2,\mu,-\sigma}^\dagger, \end{aligned} \quad (9)$$

which is another B_{1g} intra-orbital pairing operator with the two particles located in the same orbital but at different oxygens [see panel (b) in Fig. 3] and it is analogous to the extended, nearest-neighbor, *s*-wave operator defined in the context of the cuprates [29, 35]. In addition, the commutator between Δ_{Dpd}^\dagger and the t_{pp} hopping term in H_{3BH} leads to an extended version of Δ_{Dpd}^\dagger that forms pairs with one fermion on a *d* orbital at site \mathbf{r} and the other at orbital p_x (p_y) at distance $\mathbf{r} + \mathbf{y} + \mathbf{x}/2$ ($\mathbf{r} + \mathbf{x} + \mathbf{y}/2$) and symmetrical points. The commutator of this extended operator with the t_{pd} hopping term in H_{3BH} finally leads to *p*-orbital pairing operators that combine fermions in p_x (p_y) orbitals along the y (x) direction which are the plaquette pairing operators mentioned

in Ref. [16] and shown in panel (d) of Fig. 3. They are given by

$$\begin{aligned} \Delta_{Dplaq}^\dagger(\mathbf{j}) &= (p_{\mathbf{j}+x/2,x,\uparrow}^\dagger p_{\mathbf{j}+y+x/2,x,\downarrow}^\dagger - \\ &\quad p_{\mathbf{j}+x/2,x,\downarrow}^\dagger p_{\mathbf{j}+y+x/2,x,\uparrow}^\dagger) - \\ &\quad (p_{\mathbf{j}+y/2,y,\uparrow}^\dagger p_{\mathbf{j}+x+y/2,y,\downarrow}^\dagger - \\ &\quad p_{\mathbf{j}+y/2,y,\downarrow}^\dagger p_{\mathbf{j}+x+y/2,y,\uparrow}^\dagger) = \\ &\quad \sum_{\mu,\sigma} f_\sigma \gamma_\mu p_{\mathbf{j}+\hat{\mu}/2,\mu,\sigma}^\dagger p_{\mathbf{j}+\bar{\mu}+\hat{\mu}/2,\mu,-\sigma}^\dagger, \end{aligned} \quad (10)$$

where $\bar{\mu} = x$ (y) if $\mu = y$ (x). We also notice that the p contribution in the standard d -wave pairing operator in Eq. (5) results from a combination of the intra-orbital p pairing operators operators Δ_{Dplaq}^\dagger and Δ_{Dpp}^\dagger .

The relationships between the minimal and the compact, but more extended, d -wave pairing operators in Fig. 3 deduced from the time-evolution calculations suggest that if the Hamiltonian indeed has a superconducting ground state with d -wave symmetry we would expect that *all* the pairing operators with that symmetry will develop long-range order simultaneously. In practice we expect the long-range behavior of local operators to be easier to study in the finite, often small, clusters accessible to numerical studies. For this reason, we will focus on the newly introduced d -wave pairing operators shown in Fig. 3 and we will compare them with the traditional ones presented in Fig. 2.

V. EFFECTIVE MODEL FOR d -WAVE PAIRING

To show explicitly that the pairing operators in Eq. (6), Eq. (8), Eq. (9), and Eq. (10) indeed lead to d -wave superconductors we will study the phenomenological Hamiltonian given by

$$H_{3BDW} = H_{TB} + H_{int}, \quad (11)$$

where the tight-binding term is the canonical of the three-orbital Hubbard model for cuprates [Eq. (2)] and the interacting portion of the Hamiltonian for the on-site same-oxygen pairing, as in D_0 , is given by

$$\begin{aligned} H_{int}^{(0)} &= - \sum_{\mathbf{j},\mu,\sigma} \gamma_\mu f(\sigma) [p_{\mathbf{j}+\hat{\mu}/2,\mu,\sigma}^\dagger p_{\mathbf{j}+\hat{\mu}/2,\mu,-\sigma}^\dagger \Delta + \\ &\quad \Delta^* p_{\mathbf{j}-\hat{\mu}/2,\mu,-\sigma} p_{\mathbf{j}-\hat{\mu}/2,\mu,\sigma}]. \end{aligned} \quad (12)$$

Δ and Δ^* are parameters that determine the strength of the superconducting condensate and they contain also the attractive coupling V usually employed in these phenomenological models. For the case of the inter-orbital extended pairing Δ_{Dpd}^\dagger the interaction term is given by

$$\begin{aligned} H_{int}^{(pd)} &= - \sum_{\mathbf{j},\mu,\sigma} \gamma_\mu f(\sigma) \alpha_{\mathbf{j},\mu} [d_{\mathbf{j},\sigma}^\dagger p_{\mathbf{j}-\hat{\mu}/2,\mu,-\sigma}^\dagger \Delta + \\ &\quad \Delta^* p_{\mathbf{j}-\hat{\mu}/2,\mu,-\sigma} d_{\mathbf{j},\sigma}]. \end{aligned} \quad (13)$$

For the intra-orbital extended pairing Δ_{Dpp}^\dagger the interaction term is given by

$$\begin{aligned} H_{int}^{(pp)} &= - \sum_{\mathbf{j},\mu,\sigma} \gamma_\mu f(\sigma) [p_{\mathbf{j}+\hat{\mu}/2,\mu,\sigma}^\dagger p_{\mathbf{j}-\hat{\mu}/2,\mu,-\sigma}^\dagger \Delta + \\ &\quad \Delta^* p_{\mathbf{j}-\hat{\mu}/2,\mu,-\sigma} p_{\mathbf{j}+\hat{\mu}/2,\mu,\sigma}], \end{aligned} \quad (14)$$

while for the plaquette operator Δ_{Dplaq}^\dagger the interaction is given by

$$\begin{aligned} H_{int}^{(plaq)} &= - \sum_{\mathbf{j},\mu,\sigma} \gamma_\mu f(\sigma) [p_{\mathbf{j}+\hat{\mu}/2,\mu,\sigma}^\dagger p_{\mathbf{j}-\hat{\mu}/2,\mu,-\sigma}^\dagger \Delta + \\ &\quad \Delta^* p_{\mathbf{j}-\hat{\mu}/2,\mu,-\sigma} p_{\mathbf{j}+\hat{\mu}/2,\mu,\sigma}]. \end{aligned} \quad (15)$$

A. Mean-Field analysis

In this section we perform a canonical mean-field analysis of the effective pairing models now using the more compact d -wave operators introduced here. As usual, via a Fourier transform we can work in momentum space which is more convenient. Thus, H_{TB} can be written as

$$H_{TB}(\mathbf{k}) = \sum_{\mathbf{k},\sigma} \Phi_{\mathbf{k},\sigma}^\dagger \xi_{\mathbf{k}} \Phi_{\mathbf{k},\sigma}, \quad (16)$$

where $\Phi_{\mathbf{k},\sigma}^\dagger = (p_x^\dagger(\mathbf{k}), p_y^\dagger(\mathbf{k}), d^\dagger(\mathbf{k}))_\sigma$ and

$$\xi_{\mathbf{k}} = \begin{pmatrix} \epsilon_p & -4t_{pp}s_x s_y & -2it_{pd}s_x \\ -4t_{pp}s_x s_y & \epsilon_p & -2it_{pd}s_y \\ 2it_{pd}s_x & 2it_{pd}s_y & 0 \end{pmatrix}, \quad (17)$$

where s_i indicates $\sin(k_i/2)$ with $i = x$ or y .

Note that in the electron representation the undoped case is characterized by one hole at the Cu and no holes at the O, which corresponds to a total of five electrons per CuO_2 unit-cell (the maximum possible electronic number in three orbitals is six). The orbital-resolved tight-binding bands along the $\Gamma - X - M - \Gamma$ path in the Brillouin zone calculated using a 100×100 square lattice (with Cu's at the sites of the lattice) is in Fig. 4. The dashed black line is the chemical potential μ_e for the important electronic density $\langle n \rangle = 5$ and the corresponding Fermi surface is in the inset. An analysis of the orbital composition of each of the three bands, shown by the color palette in the figure, indicates that the top band is purely d at the Γ point and moving away from Γ becomes hybridized with the p orbitals such that its d content becomes 78% at X and 56% at M. The two bottom bands have pure p character at the Brillouin zone center. The middle band achieves 43% d character at M, while the lower band has 21% d character at X. Note that the tight-binding Fermi surface, shown in the inset, has the qualitative form expected in the cuprates, both from the theory and experimental perspectives. However, its orbital content is only about 75% d in average, showing

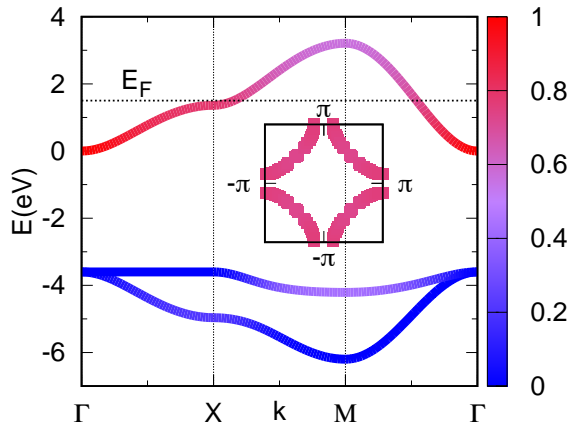


FIG. 4: (color online) Band dispersion for the tight-binding term of the CuO₂ Hamiltonian. The orbital content is displayed with red (blue) indicating *d* (*p*) character. The dashed line indicates the position of the chemical potential (or Fermi level E_F) at density $\langle n \rangle = 5$ (undoped case). The Fermi surface at this density is in the inset. Colors indicate the orbital content of the bands, with the palette on the right denoting the weight of the *d* component (e.g. 1 means 100% copper *d*, and the oxygen weight is simply one minus the copper weight).

that the oxygen component is not negligible even if only one band crosses the Fermi level.

Note that $\xi_{\mathbf{k}}$ can be written in terms of the 3×3 Gell'mann matrices [37] λ_i for the cases $i = 1$ to 8, while λ_0 is the 3×3 identity (see Appendix for an explicit form of these matrices). This is useful in order to highlight the symmetry of its different terms:

$$\xi_{\mathbf{k}} = \frac{2}{3}\epsilon_p\lambda_0 + \frac{\sqrt{3}}{3}\epsilon_p\lambda_8 + 2t_{dp}(s_x\lambda_5 + s_y\lambda_7) - 4t_{pp}s_xs_y\lambda_1. \quad (18)$$

Since the CuO₂ planes transform as D_{4h} and the Hamiltonian has to be invariant under the group operations, i.e., it has to transform as the A_{1g} representation of the group, we notice that in Eq. (18), λ_0 and λ_8 transform like A_{1g} while λ_1 transforms like B_{2g} , and (λ_5, λ_7) transform like the two-dimensional representation E_g since they are combined with (s_x, s_y) , which transforms according to E_g .

The interacting term of the Hamiltonian can be written in terms of a pairing matrix $P^{(0)}$ for the on-site same-oxygen case (Eq. (12)):

$$P_{\mathbf{k}}^{(0)} = \begin{pmatrix} 2\Delta & 0 & 0 \\ 0 & -2\Delta & 0 \\ 0 & 0 & 0 \end{pmatrix}, \quad (19)$$

which can be written in terms of the λ_i matrices as

$$P_{\mathbf{k}}^{(0)} = 2\Delta\lambda_3. \quad (20)$$

For the extended pairing (Eq. (14)) the corresponding

matrix $P^{(pp)}$ is given by

$$P_{\mathbf{k}}^{(pp)} = \begin{pmatrix} 2\Delta \cos(k_x) & 0 & 0 \\ 0 & -2\Delta \cos(k_y) & 0 \\ 0 & 0 & 0 \end{pmatrix}, \quad (21)$$

which can be written in terms of the λ_i matrices as

$$P_{\mathbf{k}}^{(pp)} = 2\Delta \left[\frac{(\cos(k_x) - \cos(k_y))}{3} \lambda_0 + \frac{(\cos(k_x) + \cos(k_y))}{2} \lambda_3 + \frac{\sqrt{3}(\cos(k_x) - \cos(k_y))}{6} \lambda_8 \right]. \quad (22)$$

For the plaquette pairing operator (Eq. (15)) the corresponding matrix $P^{(plaq)}$ is given by

$$P_{\mathbf{k}}^{(plaq)} = \begin{pmatrix} 2\Delta \cos(k_y) & 0 & 0 \\ 0 & -2\Delta \cos(k_x) & 0 \\ 0 & 0 & 0 \end{pmatrix}, \quad (23)$$

which can be written in terms of the λ_i matrices as

$$P_{\mathbf{k}}^{(plaq)} = 2\Delta \left[\frac{(\cos(k_y) - \cos(k_x))}{3} \lambda_0 + \frac{(\cos(k_y) + \cos(k_x))}{2} \lambda_3 + \frac{\sqrt{3}(\cos(k_y) - \cos(k_x))}{6} \lambda_8 \right]. \quad (24)$$

For the inter-orbital pairing operator Δ_{Dpd}^\dagger the corresponding matrix $P^{(pd)}$ (Eq. (13)) is given by

$$P_{\mathbf{k}}^{(pd)} = \begin{pmatrix} 0 & 0 & 2\Delta i s_x \\ 0 & 0 & -2\Delta i s_y \\ 2\Delta i s_x & -2\Delta i s_y & 0 \end{pmatrix}, \quad (25)$$

which can be written in terms of the λ_i matrices as

$$P_{\mathbf{k}}^{(pd)} = 2i\Delta(s_x\lambda_4 - s_y\lambda_6). \quad (26)$$

Thus, the effective interaction term can be constructed in terms of a spin-singlet pair operator that transforms according to the irreducible representation B_{1g} of D_{4h} [38]. In the case of $P^{(0)}$ the symmetry of the pairing term is given by the matrix λ_3 , which transforms according to B_{1g} . For $P^{(pp)}$ in Eq. (22) note that the terms that contain λ_0 and λ_8 , which transform like A_{1g} , are multiplied by $\cos(k_x) - \cos(k_y)$, which transforms like B_{1g} , while the term that contains λ_3 , which transforms like B_{1g} , is multiplied by $\cos(k_x) + \cos(k_y)$, which transforms like A_{1g} . A similar analysis for $P^{(plaq)}$ in Eq. (24) shows that it also transforms like B_{1g} . The inter-orbital pairing operator also transforms as B_{1g} because it combines (s_x, s_y) with (λ_4, λ_6) each transforming like E_g . Finally, for completeness, we present the pairing matrices for the traditional *d*-wave operator of the single and three-orbital Hubbard models presented in Eq. (4) and Eq. (5). For Δ_D^\dagger the corresponding matrix $P^{(D)}$ is

$$P_{\mathbf{k}}^{(D)} = \begin{pmatrix} 0 & 0 & 0 \\ 0 & 0 & 0 \\ 0 & 0 & 2\Delta[\cos(k_x) - \cos(k_y)] \end{pmatrix}, \quad (27)$$

which can be written in terms of the λ_i matrices as

$$P_{\mathbf{k}}^{(D)} = 2\Delta[\cos(k_x) - \cos(k_y)](\lambda_0 - \sqrt{3}\lambda_8), \quad (28)$$

and for Δ_{D3B}^\dagger the corresponding matrix $P^{(D3B)}$ is

$$P_{\mathbf{k}}^{(D3B)} = 2\Delta[\cos(k_x) - \cos(k_y)] \begin{pmatrix} 1 & 0 & 0 \\ 0 & 1 & 0 \\ 0 & 0 & 1 \end{pmatrix}, \quad (29)$$

which can be written in terms of the λ_i matrices as

$$P_{\mathbf{k}}^{(D3B)} = 2\Delta[\cos(k_x) - \cos(k_y)]\lambda_0. \quad (30)$$

In summary, for the canonical widely used operators the B_{1g} symmetry is just directly given by the factor $\cos(k_x) - \cos(k_y)$, while for the new operators deducing the d -wave character requires a careful analysis.

Another way of verifying the d -wave symmetry of the proposed pairing operators is the calculation of the band structure via the resulting 6×6 Bogoliubov-de Gennes Hamiltonian given by

$$H_{\text{BdG}} = \sum_{\mathbf{k}} \Psi_{\mathbf{k}}^\dagger H_{\mathbf{k}}^{\text{MF}} \Psi_{\mathbf{k}}, \quad (31)$$

with the definitions

$$\Psi_{\mathbf{k}}^\dagger = (p_{\mathbf{k},x,\uparrow}^\dagger, p_{\mathbf{k},y,\uparrow}^\dagger, d_{\mathbf{k},\uparrow}^\dagger, p_{-\mathbf{k},x,\downarrow}, p_{-\mathbf{k},y,\downarrow}, d_{-\mathbf{k},\downarrow}), \quad (32)$$

and

$$H_{\mathbf{k}}^{\text{MF}} = \begin{pmatrix} (H_{\text{TB}}(\mathbf{k}) - \mu_e \lambda_0) & P^{(\alpha)}(\mathbf{k}) \\ (P^{(\alpha)})^\dagger(\mathbf{k}) & -(H_{\text{TB}}(\mathbf{k}) - \mu_e \lambda_0) \end{pmatrix}, \quad (33)$$

where the label α takes the values 0, pp , pd , $plaq$, D , or $D3B$, and we have included the chemical potential μ_e into the tight-binding term to ensure that the gap opens at the Fermi surface.

Diagonalizing the mean-field Hamiltonian we find that a d -wave gap opens at the chemical potential. The resulting band structures for $\alpha = 0$ and pp are shown in Fig. 5 for a 100×100 lattice at a density of 4.9 electrons per unit cell (5 electrons per unit cell corresponds to the undoped case) along the main directions in momentum space for various values of Δ . Results for $\Delta = 0$ are shown to indicate the non-interacting Fermi surface. The results for the on-site pairing operator D_0 ($\alpha = 0$) are shown in panel (a) of the figure, while those for the extended operator D_{pp} ($\alpha = pp$) are in panel (b). In panels (c) and (d) it can be seen that for both $\Delta = 0.3$ and 0.5 a gap opens at the antinodal position X but the node along the diagonal direction $\Gamma - M$ remains, indicating the d -wave symmetry of the gap, as expected. In addition, note that the interaction only distorts the bands close to the Fermi surface and we observe a very flat dispersion of the band that defines the gap at X , in agreement with recent experiments [16]. The results for the plaquette, inter-orbital, and traditional operators look very similar and are not shown explicitly.

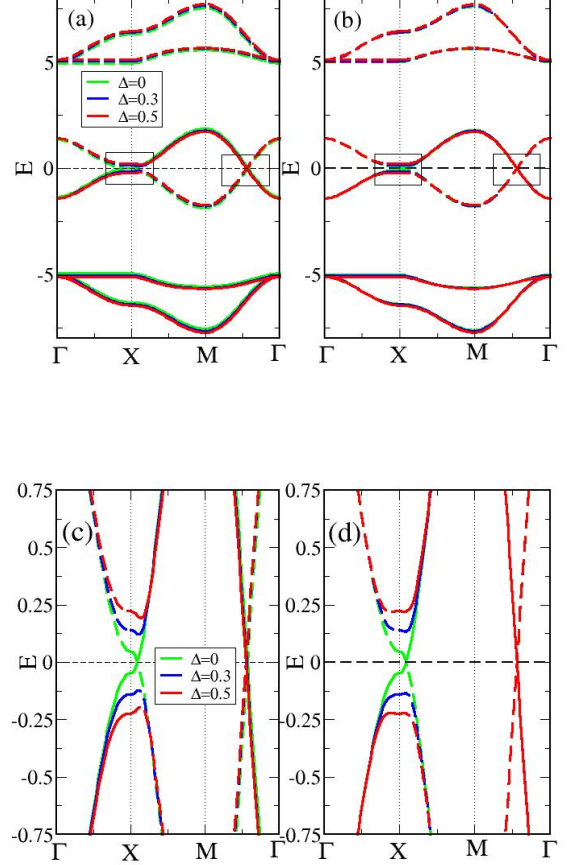


FIG. 5: (color online) Band dispersion for the mean-field Hamiltonians with B_{1g} pairing. (a) corresponds to on-site D_0 and (b) to extended D_{pp} , for the indicated values of the pairing order parameter Δ at a density of 4.9 electrons per unit cell; (c) detail of the areas inside rectangular boxes in (a); (d) detail of the areas inside rectangular boxes in (b). The dashed lines indicate “shadow” bands.

B. Stability of d -wave state

The next aspect to explore is the stability of the pairing state with a finite gap. To study this issue we need to evaluate the energy of the mean-field Hamiltonian vs Δ for different values of the pairing strength V , where $\Delta = V \langle p_{-\mathbf{k},\mu,\downarrow} p_{\mathbf{k},\mu,\uparrow} \rangle$ for the on-site pairing D_0 , which we assume is the same for all values of μ . The total energy is

$$E = \sum_{\mathbf{k}} \left[\sum_{i=1}^3 (\epsilon_i(\mathbf{k}) - \mu_e) - E_i(\mathbf{k}) \right] + \frac{\Delta^2 N}{V}, \quad (34)$$

where $\epsilon_i(\mathbf{k})$ are the eigenvalues of the tight-binding term, E_i are the three negative eigenvalues of the mean-field matrix (where the chemical potential has been included), and N is the number of sites of the large but finite cluster used. The appropriate fermionic operators need to be

Operator label	$V_{\Delta=20 \text{ meV}} \text{ (eV)}$
D_0	2.38
D_{pp}	3.68
D_{plaq}	3.50
D_{pd}	0.50
D_D	0.13
D_{D3B}	0.15

TABLE I: $V_{\Delta=20 \text{ meV}}$ indicates the value of the attraction that produces a total gap of 40 meV for the corresponding d -wave pairing.

used in the expression of Δ for the remaining d -wave pairing operators.

We have observed that any finite value of V stabilizes the proposed pairing states, similar to what happens in the negative- U Hubbard model. The small values of Δ that minimizes the energy for the different values of V are indicated with an arrow in panels (a) and (b) of Fig. 6 for the pairing operators D_0 and D_{pp} . Experimentally, the value of the superconducting gap in the cuprates ranges from 20 meV to 40 meV [39]. Since the gap in our model is equal to 2Δ we see from the figure that $V \sim 2.4$ ($V \sim 3.6$) provides a reasonable value of Δ for the minimum energy for on-site (extended) pairing. While all

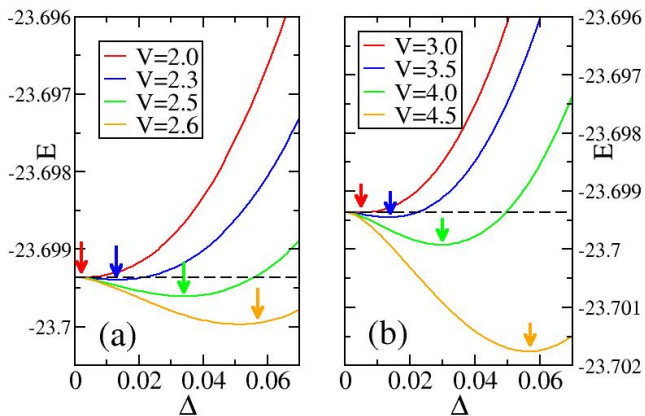


FIG. 6: (color online) Total energy versus Δ at various values of V for (a) the on-site D_0 and (b) the extended D_{pp} pairing operators. Arrows indicate the minima in the energies. Δ and E are in units of eV.

the d -wave pairing operators open a gap in the density of states as soon as V is finite, we observed that all the pairing states that include d -orbitals produce larger gaps than the pure p -orbital operators at a fixed value of the attraction V . This becomes clear as we obtain the value of V needed in each case to open a gap similar to the one observed in the cuprates. In Table I we present the values of the attraction that stabilizes a gap of 20 meV in each case, and it can be seen that $V < 1 \text{ eV}$ ($V > 1 \text{ eV}$) is needed for operators that (do not) involve d -orbitals.

Thus, the mean-field results appear to indicate that

pairing operators that involve the d -orbital need a much smaller attraction to produce a superconducting gap similar to the one observed in the cuprates. This is probably due to the fact that in the mean-field calculations the gap opens around the non-interacting Fermi surface which, as shown in Fig. 4, it is mostly a d -band. In the cuprates though, it is expected that the band that forms the non-interacting Fermi surface would generate upper and lower bands, due to the Coulomb repulsion at the Cu, and the Fermi surface upon doping will occur in a $p-d$ hybridized band, identified as a Zhang-Rice band in photoemission [40]. Due to the higher weight of the p -orbitals in this band, it is expected that the p -based compact d -wave order parameters proposed here may work better than the traditionally used pairing operators.

VI. PHENOMENOLOGICAL MODEL

Finally, if we replace Δ by $2V\gamma_\nu p_{\mathbf{j}+\hat{\nu}/2,\nu,\downarrow} p_{\mathbf{j}+\hat{\nu}/2,\nu,\uparrow}$ instead of the average value of the pairing operator in Eq. (12), we obtain a phenomenological interaction that should promote the on-site d -wave pairing D_0 given by:

$$\begin{aligned}
 H_{\text{int}} = & \\
 & -4V \sum_{\mathbf{j},\mu,\nu} \gamma_\mu \gamma_\nu p_{\mathbf{j}+\hat{\mu}/2,\mu,\uparrow}^\dagger p_{\mathbf{j}+\hat{\mu}/2,\mu,\downarrow}^\dagger p_{\mathbf{j}+\hat{\nu}/2,\nu,\downarrow} p_{\mathbf{j}+\hat{\nu}/2,\nu,\uparrow} = \\
 & -4V \sum_{\mathbf{j},\mu} n_{\mathbf{j}+\hat{\mu}/2,\mu,\uparrow} n_{\mathbf{j}+\hat{\mu}/2,\mu,\downarrow} + \\
 & 4V \sum_{\mathbf{j},\mu \neq \nu} p_{\mathbf{j}+\hat{\mu}/2,\mu,\uparrow}^\dagger p_{\mathbf{j}+\hat{\nu}/2,\nu,\downarrow}^\dagger p_{\mathbf{j}+\hat{\mu}/2,\mu,\downarrow} p_{\mathbf{j}+\hat{\nu}/2,\nu,\uparrow}.
 \end{aligned} \tag{35}$$

The first term is an effective on-site attraction in the O sites while the second term involves the four O's that surround the Cu at site \mathbf{j} and is repulsive. While it is unlikely that terms of this form could be dynamically generated by the long-range Coulomb repulsion and a short-range attraction induced by antiferromagnetic fluctuations, it is important to remember that the electron-phonon interaction in BCS superconductors does not lead to the instantaneous on-site attraction of the negative- U Hubbard model. However, this model has been an important phenomenological tool to study the behavior of s -wave superconductors, both with weak and strong attraction. Then, it is possible that the Hamiltonian here proposed could play a similar role but for d -wave superconductors. In order to observe long-range order with this very local pairing operator it may be necessary to use a considerably large value of V to allow for a higher $p-d$ hybridization at the Fermi surface.

VII. CONCLUSIONS

Summarizing, in this effort new intracell-CuO₂ – three intra-orbital and one inter-orbital – pairing operators

with d -wave symmetry have been proposed for the high critical temperature cuprates. These operators are more local (more compact in size) than those previously employed in numerical studies and, thus, they may produce a stronger signal when their long-range behavior in finite systems is studied with numerical many-body techniques. In addition, they may be able to account for the small size of the pairs recently experimentally observed in the cuprates via angle-resolved photoemission methods. At the mean-field level, the flatness of the band that forms the gap at the antinodes is reproduced and it is demonstrated that the size of the superconducting gap experimentally observed is obtained even with a moderate attraction [41]. The next step would be to evaluate more properties of these pairing operators at the mean-field level and, even more importantly, to calculate their pairing correlations in the three-orbital Hubbard model employing unbiased computational techniques.

VIII. ACKNOWLEDGMENTS

The authors were supported by the U.S. Department of Energy (DOE), Office of Science, Basic Energy Sciences (BES), Materials Sciences and Engineering Division.

Appendix A: λ_i matrices

The λ_i matrices used in the text are presented here:

$$\lambda_0 = \begin{pmatrix} 1 & 0 & 0 \\ 0 & 1 & 0 \\ 0 & 0 & 1 \end{pmatrix}, \quad \lambda_1 = \begin{pmatrix} 0 & 1 & 0 \\ 1 & 0 & 0 \\ 0 & 0 & 0 \end{pmatrix},$$

$$\lambda_2 = \begin{pmatrix} 0 & -i & 0 \\ i & 0 & 0 \\ 0 & 0 & 0 \end{pmatrix}, \quad \lambda_3 = \begin{pmatrix} 1 & 0 & 0 \\ 0 & -1 & 0 \\ 0 & 0 & 0 \end{pmatrix},$$

$$\lambda_4 = \begin{pmatrix} 0 & 0 & 1 \\ 0 & 0 & 0 \\ 1 & 0 & 0 \end{pmatrix}, \quad \lambda_5 = \begin{pmatrix} 0 & 0 & -i \\ 0 & 0 & 0 \\ i & 0 & 0 \end{pmatrix},$$

$$\lambda_6 = \begin{pmatrix} 0 & 0 & 0 \\ 0 & 0 & 1 \\ 0 & 1 & 0 \end{pmatrix}, \quad \lambda_7 = \begin{pmatrix} 0 & 0 & 0 \\ 0 & 0 & -i \\ 0 & i & 0 \end{pmatrix},$$

$$\lambda_8 = \frac{1}{\sqrt{3}} \begin{pmatrix} 1 & 0 & 0 \\ 0 & 1 & 0 \\ 0 & 0 & -2 \end{pmatrix}.$$

-
- [1] C. C. Tsuei, J. R. Kirtley, C. C. Chi, Lock See Yu-Jahnes, A. Gupta, T. Shaw, J. Z. Sun, and M. B. Ketchen, Phys. Rev. Lett. **73**, 593 (1994).
- [2] J. R. Kirtley, C. C. Tsuei, J. Z. Sun, C. C. Chi, L. S. Yu-Jahnes, A. Gupta, M. Rupp, and M. B. Ketchen, Nature (London) **373**, 225 (1995).
- [3] R. T. Scalettar, E. Y. Loh, J. E. Gubernatis, A. Moreo, S. R. White, D. J. Scalapino, R. L. Sugar, and E. Dagotto, Phys. Rev. Lett. **62**, 1407 (1989).
- [4] A. Moreo and D. J. Scalapino, Phys. Rev. Lett. **66**, 946 (1991).
- [5] M. Randeria, N. Trivedi, A. Moreo, and R. T. Scalettar, Phys. Rev. Lett. **69**, 2001 (1992).
- [6] E. Dagotto, J. Riera, Y. C. Chen, A. Moreo, A. Nazarenko, F. Alcaraz, and F. Ortolani, Phys. Rev. B **49**, 3548 (1994).
- [7] A. Nazarenko, A. Moreo, E. Dagotto, and J. Riera, Phys. Rev. B **54**, R768 (1996).
- [8] D. S. Rokhsar and S. A. Kivelson, Phys. Rev. Lett. **61**, 2376 (1988).
- [9] F. F. Assaad, M. Imada, and D. J. Scalapino, Phys. Rev. Lett. **77**, 4592 (1996).
- [10] Phenomenologically, the coupling of fermions with classical pairing fields leads to d -wave pairing, see M. Mayr, G. Alvarez, C. Sen, and E. Dagotto, Phys. Rev. Lett. **94**, 217001 (2005), but we are searching for purely fermionic systems.
- [11] D. C. Johnston, Adv. Phys. **59**, 803 (2010).
- [12] P. Dai, J. P. Hu, and E. Dagotto, Nat. Phys. **8**, 709 (2012).
- [13] Y. Wan and Q.-H. Wang, Europhys. Lett. **85**, 57007 (2009).
- [14] M. Daghofer, A. Moreo, J. A. Riera, E. Arrigoni, D. J. Scalapino, and E. Dagotto, Phys. Rev. Lett. **101**, 237004 (2008).
- [15] C. B. Bishop, G. Liu, E. Dagotto, and A. Moreo, Phys. Rev. B **93**, 224519 (2016).
- [16] H. Li, X. Zhou, S. Parham, K. N. Gordon, R. D. Zhong, J. Schneeloch, G. D. Gu, Y. Huang, H. Berger, G. B. Arnold, and D. S. Dessau, arXiv:1809.02194.
- [17] M. S. D. A. Hussein, E. Dagotto, and A. Moreo, Phys. Rev. B **99**, 110158 (2019).
- [18] E. Arrigoni, M. Aichhorn, M. Daghofer, and W. Hanke, New J. Phys. **11**, 055066 (2009).
- [19] E. W. Huang, C. B. Mendl, S. Liu, S. Johnston, H.-C. Jiang, B. Moritz, and T. P. Devereaux, Science **358**, 1161 (2017).
- [20] E. Dagotto and J. R. Schrieffer, Phys. Rev. B **43** (RC), 8705 (1991).
- [21] V. J. Emery and G. Reiter, Phys. Rev. B **38**, 11938(R) (1988).
- [22] M. S. Hybertsen, M. Schlüter, and N. E. Christensen, Phys. Rev. B **39**, 9028 (1989).
- [23] M. S. D. A. Hussein, M. Daghofer, E. Dagotto, and A. Moreo, Phys. Rev. B **98**, 035124 (2018).
- [24] Z.-X. Shen, J. W. Allen, J. J. Yeh, J.-S. Kang, W. Ellis,

- W. Spicer, I. Lindau, M. B. Maple, Y. D. Dalichaouch, M. S. Torikachvili, J. Z. Sun, and T. H. Geballe, Phys. Rev. B **36**, 8414 (1987).
- [25] J. W. Allen, C. G. Olson, M. B. Maple, J.-S. Kang, L. Z. Liu, J.-H. Park, R. O. Anderson, W. P. Ellis, J. T. Markert, Y. Dalichaouch, and R. Liu, Phys. Rev. Lett. **64**, 595 (1990).
- [26] B. O. Wells, Z.-X. Shen, A. Matsuura, D. M. King, M. A. Kastner, M. Greven, and R. J. Birgeneau, Phys. Rev. Lett. **74**, 964 (1995).
- [27] A. Damascelli, Z. Hussain, and Z.-X. Shen, Rev. Mod. Phys. **75**, 473 (2003).
- [28] F. C. Zhang and T. M. Rice, Phys. Rev. B **37**, 3759 (1988).
- [29] E. Dagotto, Rev. Mod. Phys. **66**, 763 (1994).
- [30] D. J. Scalapino, Phys. Reports **250**, 329 (1995).
- [31] G. Dopf, A. Muramatsu, and W. Hanke, Phys. Rev. B **41**, 9264 (1990).
- [32] Z. B. Huang, H. Q. Lin, and J. E. Gubernatis, Phys. Rev. B **63**, 115112 (2001).
- [33] P. B. Littlewood and C. M. Varma, Phys. Rev. Lett. **63**, 2602 (1989).
- [34] C. D. Batista and A. A. Aligia, Phys. Rev. B **48**, 4212(R) (1993).
- [35] S. Zhang, Phys. Rev. B **42**, 1012(R) (1990).
- [36] W.-L. You, S.-J. Gu, G.-S. Tian, and H.-Q. Lin, Phys. Rev. B **79**, 014508 (2009).
- [37] L. Schiff, *Quantum Mechanics*, third ed. (McGraw-Hill Kogakusha, Tokyo, 1968).
- [38] M. Daghofer, A. Nicholson, A. Moreo, and E. Dagotto. Phys. Rev. B **81**, 014511 (2010).
- [39] T. Yoshida¹, M. Hashimoto, I. M. Vishik, Z.-X. Shen, and A. Fujimori, J. Phys. Soc. Jpn. **81**, 011006 (2012).
- [40] J.G. Zaanen, G.A. Sawatzky, and J.W. Allen, Phys. Rev. Lett. **55**, 418 (1985).
- [41] While in BCS superconductors an infinitesimal attraction stabilizes the superconducting state, this may not be the case in the cuprates and, in addition, when the Coulomb interaction is taken into account the orbital content at the chemical potential for a doped system will contain more p contributions than in the non-interacting case.